Arab Journal of Nuclear Sciences and Applications

Removal of Chromium from Liquid Waste by Gamma Aluminum Oxide (γ-Al₂O₃) Nanoparticles Synthesized Using Citrate Sol-gel Method

W.M.Abdellah[1] , E.S. Abdelfattah[1], H.M.Diab[1], and E.A. Saad [2]

[1]*The Egyptian Nuclear and Radiological Regulatory Authority, Cairo, Egypt [2]Radiation Protection Department,*
[2]*Chemistry Department, Faculty of Science, Ain Shams University, Cairo, Egypt*

Gamma Aluminum oxide (γ-Al₂O₃) nanoparticles, of a particle size less than 8 nm, were synthesized from aluminum nitrate nonahydrate and citric acid via a citrate sol-gel method. The prepared alumina products were characterized by means of X-Ray Diffraction (XRD), Fourier Transform Infrared Spectroscopy (FTIR), Field Emission Scanning Electron Microscope (FE-SEM) and High Resolution Transmission Electron Microscope (HR-TEM). Different phases of alumina like amorphous, γ-Al₂O₃ and α/γ-Al₂O₃ nanoparticles were obtained on changing the calcination temperature for the alumina samples. The adsorption properties of the active p hase γ-Al₂O₃ for the removal of Cr(VI) from liquid waste were examined by batch adsorption study. The effect of different parameters such as the initial pH value, contact time and temperature on the adsorption performance of Cr (VI) onto γ-Al₂O₃ was studied. The adsorption process reached the equilibrium after 75 min and was found to be maximum at pH=3. The removal efficiency percentage of Cr(VI) using γ-Al₂O₃ was found to increase with the increase in temperature. The equilibrium adsorption was described using Langmuir model and the adsorption kinetics fits well the pseudo- second order model.

Keywords: γ-Al₂O₃/ Nanostructures/Cr(VI) /Citrate Sol-gel /Synthesis/Adsorption

Introduction

Recently much attention has been paid to the environment so as to keep it clean and free from toxic heavy metals such as chromium which is used in various applications. These include paints, fertilizer industries, leather tanning, metal polishing, electroplating, textiles metal cleaning and plating baths etc.[1-3]. On the other hand, the rapidly increasing use of nuclear power and the different applications of radionuclides in numerous fields such as medicine, agriculture, industry and research result in large amounts of radioactive waste. In particular, radioactive chromium-51, which is used widely in medicine can cause a remarkable impact on the environment and can pose serious chemical and radiological toxicity, representing a severe human health hazards [4] .

Different treatment techniques have been applied for separation of radionuclides from liquid waste.

These include chemical precipitation, evaporation, solvent extraction, membrane processes and adsorption. The adsorption technique still has the superiority over all other methods due to its simplicity, high efficiency, cheapness, and regeneration of the adsorbents [5].

In the last few years, a great scientific interest has been paid to utilize nano-adsorbents for treating of wastewater because of their high surface area, large numbers of active sites, and high stability [6]. Among the available adsorbents, Nanosized Metal Oxides (NMO's) including nanosized Al₂O₃, that classified as the promising material for chromium removal from aquatic environment systems [7].

Nanocrystalline alumina can be obtained utilizing various processes such as precipitation, gas phase

deposition, sol–gel, hydrothermal and combustion methods [8]. Sol-gel synthesis is a fast and effective method for producing fine and homogeneous Nano-sized oxide powders and alumina [9-11].

The aim of the presentworkis the synthesis of low cost adsorbent γ- Al_2O_3 nanoparticles using citrate sol–gel method and to study the effect of different calcination temperatures on the crystal size and the produced phase. Moreover, removal of chromium Cr(VI) using the prepared γ-Al_2O_3 nanostructures has been investigated. Various experimental factors influencing the adsorption process along with the isotherm models, kinetics and thermodynamic have been examined.

Experimental

Materials and reagents
All chemicals were analytical grade, purchased and used as received without further purification: aluminum nitrate of the $Al(NO_3)_3.9H_2O$,Merck, citric acid $(HOC(COOH)(CH_2COOH)_2$; Sigma–Aldrich Chemical Co., ammonium hydroxide 25% NH_3 in H_2O; Sigma–Aldrich Chemical Co., and Potassium dichromate $(K_2Cr_2O_7)$ from Merck.

Preparation γ-Al_2O_3 nanostructures
Gamma aluminum oxide nanostructures were synthesized via the citrate sol-gel method in which citric acid was used as a chelating agent. In thepreparation procedure, an aqueous solution of aluminum nitrate was heated up to 60 °C, with stirring for 10 min. An aqueous solution of citric acid was addedand heated at 80 °C with stirring for one hour. The produced solution was dried at 200 °C for 2 h. Thedried material was ground and calcined at various temperatures 500,600,800 and 1000 °C to give Al_2O_3 nanostructures referred as (A_{500}, B_{600}, C_{800} and D_{1000}).

Physico-chemical measurements
The prepared nano alumina will be characterized and identified using different techniques as follows:
- *X-Ray Diffraction (XRD) technique,* was employed to study the phase composition of the synthesized nano particles, using 18 kW diffractometer (Bruker; model D8 Advance) with mono-chromated Cu Ka radiation (l) 1.54178 Å).

- *Fourier Transform Infrared Spectroscopy (FTIR)*,spectra were recorded using FT-IR spectrometer (Bomem; model MB157S) in the range of 4000-400 cm^{-1} at room temperature.
- *Morphology Study:* to investigate the morphology and the particle diameter of the produced samples the following techniques were used.a) Field Emission Scanning Electron Microscope (FE-SEM) with a microscope (JEOL JSM-6510LA), at a speeding voltage of 30 kV. B) High Resolution Transmission Electron Microscope (HRTEM): model (TEM-2100) at a speeding voltage of 200 kV was used for imaging by dispersing the sample in ethanol on a copper grid
- UV-Visible. Spectrophotometer model (UnicamUV-540) was used during adsorption investigation.

Adsorption Process
50 mg of γ-Al_2O_3 nanoparticles in (25 mL) of 20 ppm of $K_2Cr_2O_7$ solution was stirred at room temperature (25 ℃)at equilibrium time,then centrifuged at 4000 rpm. The concentration of the remaining Cr(VI), in the supernatant was estimated spectrophotometrically by developing a purple-violet color with 1,5-Di-Phenyl Carbazide (DPC) in acidic solution, at 540 nm.The adsorption capacity of the adsorbent (q_t, mg/g) was calculated using equation (1). Moreover, the removal percentage of (%R) of the Cr(VI) was determined using equation (2).

$$q_t = (C_0 - C_t) \times \frac{V}{m} \qquad (1)$$

Where, C_0 (mg/L) is the initial Cr(VI) concentration, C_t (mg/L) is the chromium concentration in solution at equilibrium time t, V(L) is the volume of the $K_2Cr_2O_7$ solution, and m(g) is the mass of the γ-aluminum oxide adsorbent.

$$Cr(VI)R\% = \frac{(C_0 - C_t)}{C_0} \times 100 \qquad (2)$$

Various factors have been investigated such as contact time (15-90 min), pH(2-9), temperature (25-55℃) and initial Cr(VI) concentration (10-50 mg/L). The equilibrium adsorption capacity of γ-Al_2O_3 adsorbent, q_e (mg/g), was determinedusing equation (3).

$$q_e = (C_0 - C_e) \times \frac{V}{m} \qquad (3)$$

where, C_e (mg/L) is the Cr(VI) concentration at equilibrium in the supernatant after separation of the adsorbent.

RESULTS AND DISCUSSION

X-Ray diffraction (XRD) analysis

It is obvious from Fig. 1curve (A) that the calcinated temperature at 500°C was not enough to produce a crystalline product and the amorphous character of the powder is evidenced. If the temperature is increased to 600°C,a broad diffraction pattern was producedas shown in Fig. 1curve(B) for sample B_{600}, whichcharacteristic ofγ-$Al_2O_3$and indexed to the standard card No[JCPDS No. 10-0425]. It is noticed that raising the temperature to 800°C increasethe diffraction pattern of the gamma phase for Sample C_{800} which fitted to card [JCPDS No. 10-0425]. When the temperature was increased to 1000 ^{o}C, the crystallinity of γ-Al_2O_3 increased as shown in Fig. (1) curve (D). The obtained results reveal a sharp diffraction peak which characterizes the alpha-Al_2O_3 beside the broad one for gamma-Al_2O_3.

The Debye-Scherer equation (4) [12], was applied to calculate the crystallite size (D, nm) for the obtained aluminum oxide nanoparticles as follows:

$$D = \frac{0.9\lambda}{\beta \cos\theta B} \tag{4}$$

Where, λ (nm) is the X-ray radiation wavelength, β is the diffraction peak full width at half maximum (FWHM), and θB is the Bragg diffraction angle. The average crystallite size of the prepared aluminum oxide nanoparticles was about (3.95 nm), (7.15 nm) and (21.72 nm) at 600,800 and 1000°C respectively. It can be concluded that changing the calcination temperature has a remarkable effect on both the particle size and the phase of the synthesized nano-alumina.
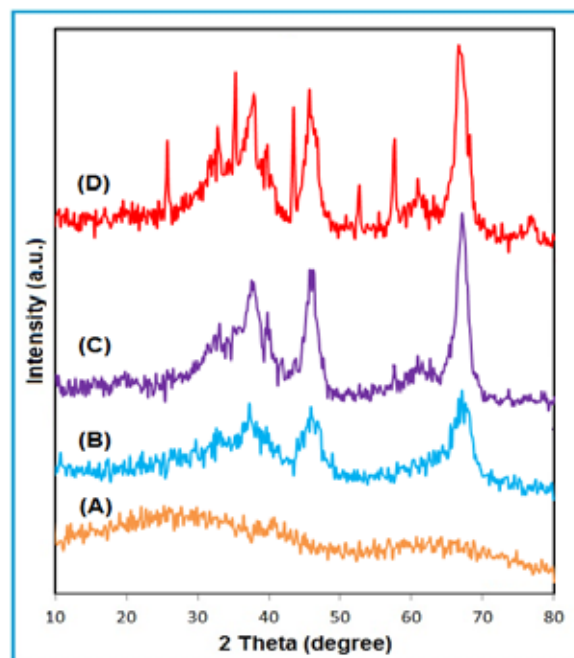

Fig. (1): XRD patterns of γ-Al_2O_3 samples A, B, C, and D calcined at 500,600,800 and 1000 ^{o}C respectively

FT-IR analysis

The FTIR spectra of the prepared γ-Al_2O_3 nanoparticles is shown in Fig. 2. The broad peak at 3480 cm^{-1} and the band at 1635 cm^{-1} can be attributed to the stretching and bending modes of the adsorbed water, respectively [13]. Absorption peaks around 2350 cm^{-1} related to the stretching vibration of HCO_3^- group may due to absorption of CO_2 from air during preparing the samples [14]. The shape and relative intensity of absorption bands in the region of 400–900 cm^{-1} represent a variety of Al-oxide bonds [15] and in general, related to stretching vibration of Al–O bonds which confirms the formation of gamma phase [16].
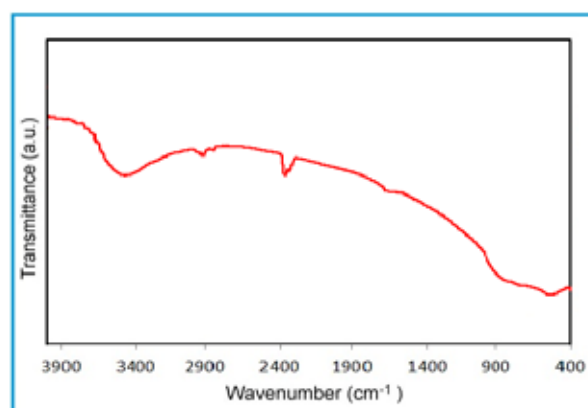

Fig. (2): FT-IR spectra of γ-Al_2O_3 product calcined at 800 ^{o}C

Morphology study
Field Emission Scanning Electron Microscopy (FE-SEM) image of γ-Al_2O_3 sample C_{800} is represented in Fig. (3). It shows aggregates of solid blocks of irregular-shapes of γ-Al_2O_3 subcrystals and some crystals of thin layers or sheets-like structure of γ-Al_2O_3.
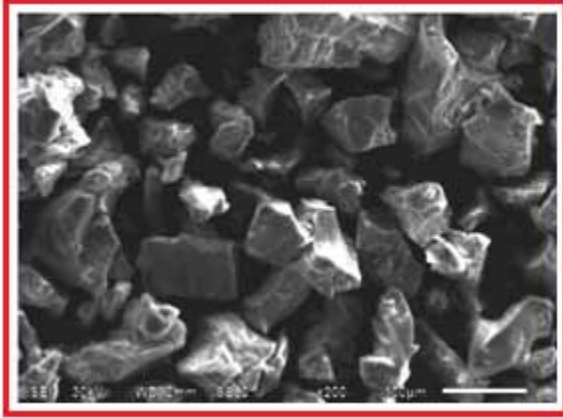

Fig. (3): FE-SEM image of γ-Al_2O_3 product calcined at 800 ⁰C

HR-TEM image of γ-Al_2O_3 sample C_{800}, shown in Fig. (4) reveals dense bulk agglomerates of a very small sphere-like and irregular shapes of the alumina particles and these agglomerates may be attributed to the small and very fine alumina particles. With an average diameter of 8 nm, which is consistent well with the crystallite size, calculated from the XRD studies.
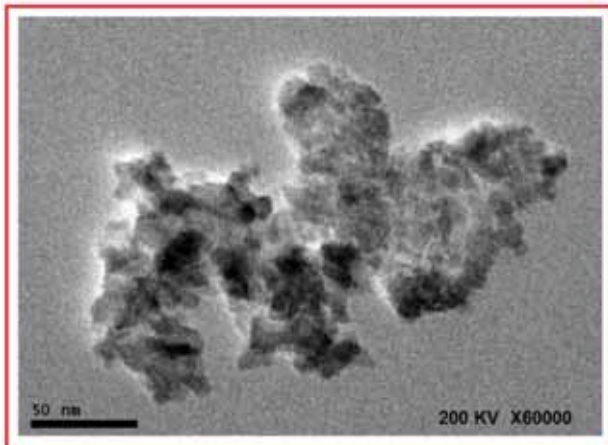

Fig. (4): HR-TEM image of γ-Al_2O_3 product calcined at 800 ⁰C

Adsorption of chromium ion on γ-Al_2O_3 nanoparticles
a) Effect of pH
   Fig. (5) illustrats that the Cr(VI) adsorption on γ-Al_2O_3 is decreased with increasing pH value, the

maximum adsorption percentage was 95.3% at pH 3. This behavior can be explained by taking into account the surface charge of γ-Al_2O_3 nanoparticles and Cr(VI) ions at different pH values. At lower pH values, γ-Al_2O_3 particles surfaces will be probably covered by protons forming positively charged particles and Cr(VI) is dominantly present as $HCrO_4^{-1}$, resulting into increased electrostatic interaction between negative Cr(VI) species and positive surface of the adsorbent [17]. While at higher pH values, there is a remarkable decrease in Cr(VI) removal which may be attributed to electrostatic repulsion between CrO_4^{-2} species and the negatively charged surface of the deprotonated oxide. This repulsion could be due to the reaction between the hydrous oxide and the highly concentrated hydroxide ions at alkaline solution [18].
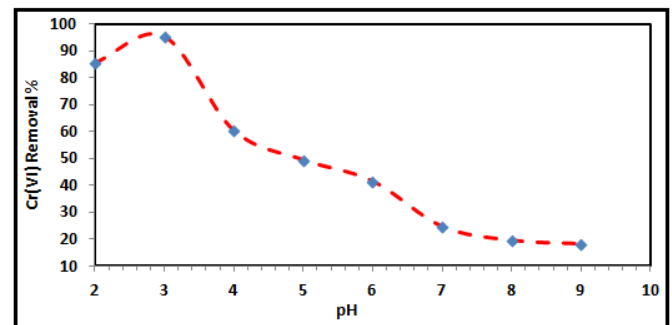

Fig. (5): Effect of pH on Cr(VI) removal percent using γ-Al_2O_3 nano-adsorbent

b) Effect of contact time
As shown in Fig. (6), the adsorption capacity of γ-Al2O3 increased rapidly in the first 15 min with a removal percentage of about 83.26 %, and then it reached 94.37%, in 75 min. The obtained data reveal that the adsorption process reached the equilibrium at 75 min and remained constant as shown in Fig. (6).
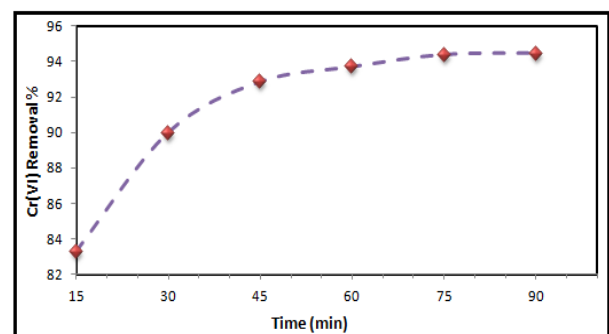

Fig. (6): Effect of contact time on Cr(VI) removal percentage using γ-Al_2O_3 nano-adsorbent

c) Effect of temperature

The removal percentage increased rapidly with increasing temperature as illustrated in Fig. (7). This indicates the endothermic process for adsorption of Cr(VI) ions on γ-Al$_2$O$_3$. The adsorbent pore size may increase at higher temperature values and, consequently, the greater active surface adsorption sites that may be available for attracting more chromium ions.
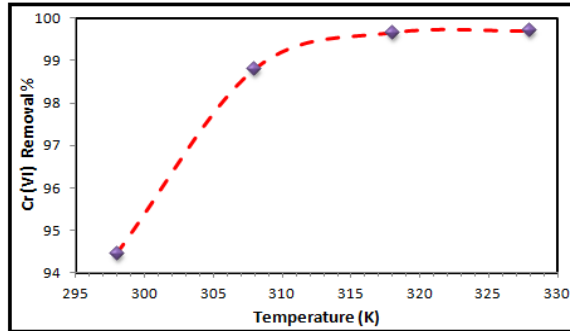

Fig. (7): Effect of temperature on Cr(VI) removal percentage using γ-Al$_2$O$_3$ nano-adsorbent

d)Effect of initial concentration

The results, in terms of removal efficiency versus initial concentration (mg/L) of Cr(VI) ions are indicated in Fig. (8). The experimental data show a significant decrease in the adsorption efficiency from 94.69 % at low concentration to 44 % at high concentration. This behavior may be due to the availability of the larger ratio of active adsorption sites of the adsorbent at lower concentration than that at high concentrations [19-21].
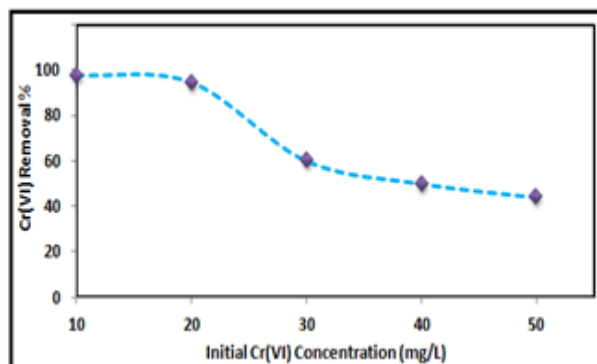

Fig. (8): Effect of initial chromium concentration Cr(VI) on the removal percentage using γ-Al$_2$O$_3$ nano-adsorbent

Adsorption isotherms study

To determine the adsorption capacity of the γ-Al$_2$O$_3$ nanoparticles, the equilibrium data for the adsorption of Cr(VI) onto γ-Al$_2$O$_3$ nanoparticles are analyzed in the light of the Langmuir and Freundlich adsorption isotherm models [22,23].

a) Langmuir isotherm model:

Langmuir isotherm model assumes the formation of a monolayer adsorbate on the outer surface of the adsorbent, and after that, no further adsorption takes place. It is valid for monolayer adsorption onto a surface containing a finite number of identical sites. The model assumes uniform energies of adsorption onto the surface and no transmigration of adsorbate in the plane of the surface. Based upon these assumptions, the linear equation of Langmuir isotherm model can be written as equation 5 [22]:

$$\frac{C_e}{q_e} = \frac{1}{Q_0 b} + \frac{C_e}{Q_0} \tag{5}$$

Where C_e is the concentration ofCr (VI) ions solution (mg/L) at equilibrium, the constant Q_0 signifies the adsorption capacity (mg/g) and b, Langmuir Constant which is related to the energy of adsorption (L/mg). Linear plot of C_e/q_e versus C_e shows Langmuir isotherm Fig. (9). Values of Q_0 and b were calculated from the slope and intercept of the linear plots as presented in Table (1). The essential characteristics of Langmuir isotherm can be expressed by a dimensionless constant called equilibrium parameter R_L, defined as follows:

$$R_L = \frac{1}{1 + bC_0} \tag{6}$$

Where b is the Langmuir constant and C_0 is the initial chromium concentration (mg/L), R_L value indicates the adsorption nature to be either unfavorable if $R_L > 1$, linear if $R_L = 1$, favorable if $0 < R_L < 1$ and irreversible if $R_L = 0$[24]. As illustrated in Table (1).The calculated R_L value is 0.039 (between zero and one) which indicates a favorable adsorption process.
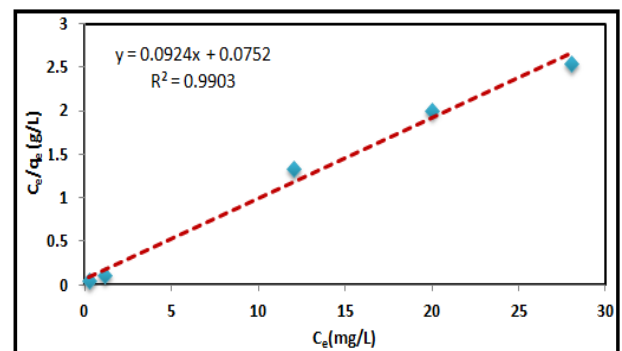

Fig. (9): Langmuir isotherm for adsorption of Cr(VI) onγ-Al$_2$O$_3$ nano-adsorbent

b) *Freundlich isotherm model*

The linearized form of the Freundlich isotherm model is based on the assumption that the adsorption takes place on a heterogeneous surface as in equation (7) [23]:

$$\ln q_e = \ln K_f + (1/n) \ln C_e \qquad (7)$$

Where, K_f is the Freundlich constant (mg/g) which represents the relative adsorption capacity of the adsorbent. (1/n) is the heterogeneity factor and it is a function of the strength of adsorption in the adsorption process and n has different values depending on the heterogeneity of the sorbent. If n lies between one and ten, this indicates a favorable sorption process [25]. The adsorption capacity of the adsorbent was studied as in Table (1). Fig. (10) and showed that, the sorption of Cr(VI) onto γ-Al₂O₃ is favorable (n=5.310). Moreover, the calculated isothermal constants shown in Table (1) indicate the adsorption of Cr(VI) ion on γ-Al₂O₃ adsorbent fits Langmuir isotherm model. In addition, the adsorption process is a monolayer coverage because the correlation coefficient (R^2) value of Langmuir isotherm is closer to unity and greater than that of Freundlich isotherm model.

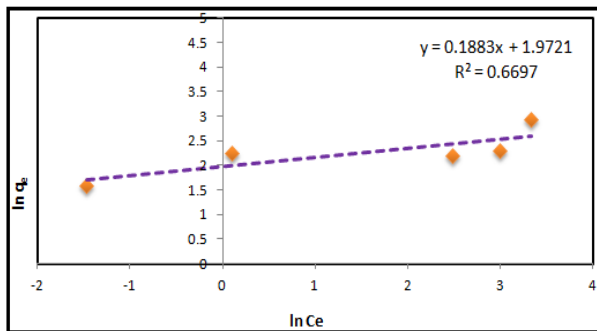*Adsorption kinetic modeling for adsorption of Cr (VI) on nanosized γ -Al₂O₃*

Fig. (10): Freundlich isotherm for adsorption of Cr(VI) onγ-Al₂O₃ nano-adsorbent

Pseudo first and pseudo second order reaction rate models were used to describe the adsorption behavior of the reaction and the rate at which the Cr(VI) ion is removed from aqueous solutions. The pseudofirstorder rate equation of Lagergen is given by equation (8) [26]:

$$\log(q_e - q_t) = \log q_e - (K_{1,ads}/2.303)t \quad (8)$$

Where q_e and q_t are the amounts of Cr(VI) ion adsorbed (mg/g) at equilibrium and at time t (min) respectively. $K_{1,ads}$ is the rate constant of pseudofirst-order adsorption (min⁻¹). Values of $K_{1,ads}$ were calculated from the plots of $\log(q_e - q_t)$ versus t (Fig. 11).
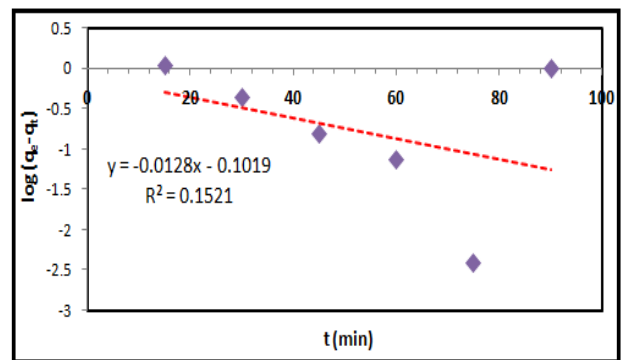

Fig. (11): Pseudo first order plots for adsorption of Cr(VI) on γ-Al₂O₃ nano-adsorbent

The rate equation for pseudo second order model is given by equation (9) [27]:

$$t/q_t = 1/(k_{2,ads}q_e^2) + (1/q_e)t \qquad (9)$$

Where $k_{2,ads}$ (g/mg. min) is the pseudo second order rate constant and its value was obtained from the plots of t/q_t versus t (Fig. 12).

Table (1): Langmuir and Freundlich Constants along with R^2 values obtained for removal of Cr(VI) on γ-Al₂O₃ nanoparticles

Pollutant	Langmuir			Freundlich		
	q_o (mg/g)	R_L (L/g)	R^2	1/n	K_F (mg/g)	R^2
Cr(VI)	10.822	0.039	0.99	0.188	7.185	0.669

Table (2) lists the rate constants, calculated equilibrium adsorption capacity q_e(cal), experimental equilibrium adsorption capacity q_e(exp), and the correlation coefficients R^2 obtained using the pseudo first and second order models. It is clearly illustrated that the adsorption of Cr(VI) ion on γ-Al$_2$O$_3$ adsorbent obeys pseudo second order model, as the value of the correlation coefficient (R^2) is close to unity when compared with that obtained from the pseudo first order model. Moreover, the value of the calculated adsorption capacity q_e(cal) employing the pseudo second order model is much closer to the experimentally obtained q_e(exp) when compared to that calculated from the pseudo first order model.

These results suggested that the pseudo secondorder adsorption mechanism is predominant and that the overall rate of the Cr(VI) ionadsorption process appeared to be controlled by the chemisorption process [28]. As γ-Al$_2$O$_3$ carries a positive charge a chemical reaction through electrostatic interaction may occur between a positive charge in the γ-Al$_2$O$_3$ particles and the negatively chargedCr(VI) ions.
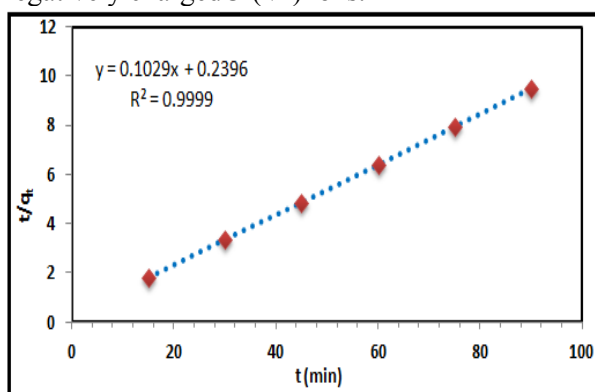

y = 0.1029x + 0.2396
R^2 = 0.9999

Fig. (12): Pseudo second-order plots for adsorption of Cr (VI) on γ-Al$_2$O$_3$ nano-adsorbent

Thermodynamic studies for adsorption of Cr(VI) on nanosized γ -Al$_2$O$_3$

The values of thermodynamic parameters such as change in enthalpy (ΔH°) and change in entropy (ΔS°) were determined using Van't Hoff equation (10) [1] and the change in free energy (ΔG°) was calculated form equation (12) as follows:

$$\ln K_d = \frac{\Delta S°}{RT} - \frac{\Delta H°}{RT} \qquad (10)$$

$$K_d = \frac{C_{Ae}}{C_e} \qquad (11)$$

$$\Delta G° = \Delta H° - T\Delta S° \qquad (12)$$

Where K_d is the equilibrium constant, C_{Ae} is the solid phase concentration at equilibrium (mg/L), T is the temperature in Kelvin and R is the gas constant (R= 8.314 x10^{-3}kJ/ Kmol). Plotting $\ln K_d$ against 1/T, as shown in Fig. (13), gives a straight line with slope and intercept equal to -ΔH° /R and ΔS°/R, respectively. The values of ΔH° and ΔS° were calculated and listed in Table (3). The positive value of ΔH° indicates the endothermic nature of Cr (VI) adsorption. The positive value of entropy change indicates an increase in the degree of freedom of the adsorbed species during adsorption process [1]. Gibbs free energy of adsorption (ΔG°) was calculated from equation (12). The negative values of ΔG° indicated the feasibility of Cr(VI) adsorption on γ-Al$_2$O$_3$. The values of ΔG° become more negative with increasing the temperature from 298 to 328 K which illustrates that the adsorption is favored at a higher temperature [29].

Table (2): Pseudo first and second order reaction rate model'sparameters for adsorption of Cr(VI) by γ-Al$_2$O$_3$ nanoparticles

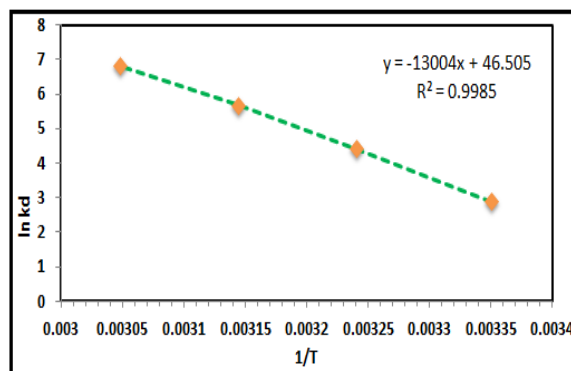| Pollutant	Pseudo first order kinetic				Pseudo second order kinetic			
	k_1 (1/min)	$q_{e(cal)}$ (mg/g)	$q_{e(exp)}$ (mg/g)	R^2	k_2 (g/mg.min)	$q_{e(cal)}$ (mg/g)	$q_{e(exp)}$ (mg/g)	R^2
Cr(VI)	0.0294	0.790	9.441	0.152	0.0497	9.157	9.441	0.999

Fig. (13): Van't Hoff plot for adsorption of Cr (VI) on γ-Al₂O₃ nano-adsorbent

Table (3): Thermodynamic parameters for adsorption of Cr (VI) on γ-Al₂O₃ nanoparticles

Tem (K)	ΔG^0 (kJ/mol)	ΔH^0 (kJ/mol)	ΔS^0 (J/mol K)
298	-7.162	108.115	0.3866
308	-11.323		
318	-15.025		
328	-18.568		

Conclusion

The prepared γ-Al2O3 nanoparticles was characterized and tested for the removal of chromium Cr(VI) from liquid waste. The removal percentage reached 94.37% at equilibrium time 75 min and optimum pH value (3). The removal efficiency was found to be increased with raising the temperature of the solution. The rate of the reaction is pseudo second order with R2 (0 .999) and the reaction follows Langmuir isotherm model with chemisorption process R2 (0 .99). The calculated positive value of enthalpy (ΔHo) indicates the endothermic nature of the reaction, and the negative value of free energy (ΔGo) illustrates that the adsorption of Cr (VI) on nano γ-Al2O3 is a spontaneous process. Finally, the present work has demonstrated that the prepared nanoparticles (γ-Al2O3) can effectively remove Cr(VI) from aqueous solutions. The obtained data of kinetic and equilibrium studies will be useful for future scale up of treating Cr(VI) rich effluent, such as electroplating or radioactive liquid waste.

References

1- W. Qiu, D. Yang, J. Xu, B. Hong, H. Jin, D. Jin, X. Peng, J. Li, H. Ge, and X. Wang, Efficient removal of Cr(VI) by magnetically separable CoFe₂O₄/activated carbon composite. *J. Alloys Compd.*, 678, 179–184 (2016).

2- X. Sun, F. Chen, J. Wei, F. Zhang, and S. Pang. Preparation of magnetic triethylene tetramine-graphene oxide ternary nanocomposite and application for Cr (VI) removal, *J. Taiwan Inst. Chem. E.*, 66, 328-335 (2016).

3- K.A. Gebru, and C. Das. Removal of chromium (VI) ions from aqueous solutions using amine-impregnated TiO₂ nanoparticles modified cellulose acetate membranes, *chemosphere*, 191, 673-684 (2018).

4- M.R. Mahmoud, and A.F. Seliman. Evaluation of silica/ferrocyanide composite as a dual-function material for simultaneous removal of $^{137}Cs^+$ and $^{99}TcO_4^-$ from aqueous solutions, *Appl. Radiat. Isot.* 91, 141–154 (2014).

5- L. Shao, X. Wang, Y. Ren, S. Wang, J. Zhong, M. Chu, H. Tang, L. Luo, and D. Xie. Facile fabrication of magnetic cucurbituril/graphene oxide composite and application for uranium removal. *Chem. Eng. J.* 286, 311–319 (2016).

6- T.H. Mahato, G.K. Prasad, B. Singh, J. Acharya, A.R. Srivastava, R. Vijayaraghavan.

Nanocrystalline zinc oxide for the decontamination of sarin, *J. Hazard. Mater. 165 928–932* (2009).

7- H.A. Dabbagh, M. Shahraki. Mesoporous nano rod-like γ-alumina synthesis using phenol-formaldehyde resin as a template, Microporous Mesoporous Mater. 175, 8–15, (2013).

8- D. Shin, S. Soo, J. Hyun, S. Soo, J. Myung, D.Ho.S. Sung, and G. Dae. Study on a -alumina precursors prepared using different ammonium salt precipitants. *J. Ind. Eng.*,20 , 1269-1275, (2013).

9- S.T. Aruna and A.S. Mukasyan. Combustion synthesis and nanomaterials, *Curr. Opin. Solid State Mater. Sci.*, 12, 44–50, (2008).

10- F. Mirjalili, M. Hasmaliza, and L.C. Abdullah. Size-controlled synthesis of nano α -alumina particles through the sol – gel method, Ceram. Int. 36, 1253–1257, (2010).

11- V.D. Zhuravlev, V.G. Bamburov, A.R. Beketov, L.A. Perelyaeva, I.V. Baklanova, O.V. Sivtsova, V.G. Vasil'Ev, E.V. Vladimirova, V.G. Shevchenko, and I.G. Grigorov. Solution combustion synthesis of α-Al₂O₃ using urea, Ceram. Int. 39, 1379–1384, (2013).

12- R. Jenkins, and R.L. Snyder. Introduction to X-ray powder diffractometry, *John Wiley & Sons, Inc., New York* (1996).

13- G. Li, Y. Liu, C. Liu. Solvothermal synthesis of gamma aluminas and their structural evolution. *Microporous Mesoporous Mater.*, 167, 137–145, (2013).

14- L. Xu, H. Song, and L. Chou. Facile synthesis of nano-crystalline alpha-alumina at low temperature via an absolute ethanol sol-gel strategy, *Mater. Chem. Phys.*, 132, 1071–1076, (2012).

15- Y. Aman, C. Rossignol, V. Garnier, and E. Djurado. Low temperature synthesis of ultrafine non vermicular α-alumina from aerosol decomposition of aluminum nitrates salts, *J. Eur. Ceram. Soc.*, 33, 1917–1928, (2013).

16- H. Yang, M. Liu, and J. Ouyang. Novel synthesis and characterization of nanosized γ-Al₂O₃ from kaolin. *Appl. Clay Sci.*, 47, 438–443 (2010).

17- Y.C. Sharma, V. Srivastava, and A.K. Mukherjee. Synthesis and application ofnano-Al₂O₃powder for the reclamation of hexavalent chromium from aqueous solutions, *J. Chem. Eng. Data* 55, 390–2398, (2010).

18- Y.S. Al-Degs, M.I. El-Barghouthi, A.H. El-Sheikh, and G.M. Walker. Effect of solution pH, ionic strength, and temperature on adsorption behavior of reactive dyes on activated carbon, *Dye. Pigment.*, 77, 16–23 (2008).

19- S. Kumararaman, K. Kirubavathi, and K. Selvaraju. Growth and characterization of l-glutamic acid hydro chloro bromide, a new nonlinear optical material, *J. Miner. Mater. Charact. Eng.*, 10, 49–57, (2011).

20- W.S.W. Nagah, and M.A. Hanafiah. Removal of heavy metal ions from wastewater by chemically modified plant wastes as adsorbents: a review, *BioresourTechnol.* , 99(10), 3935-48, (2008).

21- S. Dubey, , S.N. Upadhyay, and Y.C. Sharma. Optimization of removal of Cr by γ-alumina nano-adsorbent using response surface methodology.*Ecol. Eng.,* 97 ,272–283, (2016).

22- I. Langmuir. The adsorption of gases on plane surfaces of glass, mica and platinum, *J. Am. Chem. Soc.*, 40, 1361–1403, (1918).

23- H.M.F. Freundlich. Über die adsorption in lösungen. *Ind. Eng. Chem. Fundam.*, 57 ,385–470, (1906).

24- S. Gokila, T. Gomathi, P.N. Sudha, A. Sukumaran. Removal of the heavy metal ion chromium(VI) using Chitosan and Alginate nanocomposites, *Int. J. Biol. Macromol.,* 104, 1459–1468, (2017).

25- L. Ben Tahar, O.M. Habid, and A.A.M. Jaipallah. Synthesis of magnetite derivatives nanoparticles and their application for the removal of chromium (VI) from aqueous solutions. *J. Colloid Interface Sci.*,512, 115-126 (2017).

26- S. Dubey, D. Gusain, and Y.C. Sharma. Kinetic and isotherm parameter determination for the removal of chromium from aqueous solutions by nanoalumina, a nanoadsorbent. *J. Mol. Liq.* 219, 1–8, (2016).

27- Z. Xiao, H. Zhang, Y. Xu, M. Yuan, X. Jing, J. Huang, Q. Li, and D. Sun. Ultra-efficient removal of chromium from aqueous medium by biogenic iron based nanoparticles, *Sep. Purif. Technol.*, 174, 466–473, (2017).

28- V.K. Gupta, R. Chandra, I. Tyagi, M. Verma. Removal of hexavalent chromium ions using CuO nanoparticles for water purification applications, *J. Colloid Interface Sci.*, 478, 54–62, (2016).

29- V. Srivastava, T. Kohout, and M. Sillanpää. Potential of cobalt ferrite nanoparticles (CoFe₂O₄) for remediation of hexavalent chromium from synthetic and printing press wastewater, *J.Env. Chem.Eng.*, 4, 2922-2932, (2016).